THE ANTARES PROJECT

L. MOSCOSO *
DSM/DAPNIA, CEA/Saclay
91191 Gif-sur-Yvette CEDEX, France
E-mail: moscoso@hep.saclay.cea.fr

ABSTRACT

ANTARES is a deep-sea neutrino telescope project. Tests have been carried out over the last two years to evaluate sites, procedures and performance. The deployment of detectors and underwater electrical connections have been tested successfully at a depth of 2400 m in the Mediterranean Sea near Toulon, and the optical characteristics of the proposed site have been measured. Thanks to the good water transparency the estimated angular resolution is a few tenths of a degree allowing a very strong background suppression in the search for point sources. Moreover, new tools are in development to estimate the possibility of performing an analysis on low energy vertical neutrinos. This could allow the study of the energy spectrum between 5-10 GeV and 50 GeV, a region which is particularly sensitive to neutrino oscillations as shown by the recent results of Super-Kamiokande.

1. The ANTARES project goals

ANTARES is a project to build a deep-sea telescope for high-energy neutrino interactions. The ANTARES collaboration was formed in 1996, based on a close collaboration between particle physicists, astrophysicists, and experts in marine technology. Since then, most of the technical aspects relating to the construction and operation of this device have been addressed, and its sensitivity has been evaluated for the principal physics goals.

The ANTARES scientific program includes astrophysics (neutrino astronomy), cosmology (searches for dark matter in the form of neutralinos), and particle physics (neutrino oscillations). Neutrino astronomy provides the principal motivation for a deep-sea detector because it opens a new window for studies of the cosmos, probing regions of the universe that are opaque to photons and hadrons and energy domains well above the regime of man-made accelerators. The advantages of neutrinos are that they are electrically neutral so their trajectories will not be affected by magnetic fields, stable so that they can reach us from distant sources, and weakly interacting so that they can penetrate regions which are opaque to photons and hadrons.

The existence of astrophysical sources of high-energy neutrinos can be inferred from the existence of high-energy cosmic-ray protons. Gamma rays and neutrinos result from the decays of pions photo-produced during the acceleration of the protons. The protons are deviated by cosmic magnetic fields, but the gamma rays and neutrinos point back to their sources. Candidate sources of high-energy neutrinos

*On behalf of the ANTARES Collaboration

include galactic sources such as X-ray binaries and supernova remnants, and extra-galactic sources such as active galactic nuclei (AGN) and gamma-ray bursters (GRB). The AGN could provide a detectable source of diffuse high-energy neutrinos [1)]. Both AGN and GRB are potential point sources of high-energy neutrinos. The detection of known objects is enhanced by the excellent angular resolution expected at ANTARES.

Dark matter could be detected in high-energy neutrinos if super-symmetric neutralinos make up part of the missing mass. Relic neutralinos from the early universe would accumulate at the core of heavy bodies such as the earth, the sun, or the center of our galaxy [2)]. Because they are Majorana particles, pairs of neutralinos will annihilate. The annihilation products include neutrinos with typical energies around 1/3 to 1/2 of the neutralino mass. The angular distribution of neutrinos from neutralino annihilation in the earth's core would provide information on the neutralino mass [3)]. ANTARES would be sensitive to this effect because of its good angular resolution and its low energy threshold.

Neutrino oscillations can be studied in ANTARES with a base-line length of the order of the diameter of the earth. Atmospheric neutrinos are emitted in the decay of hadrons produced by the interaction of cosmic rays with atmospheric nuclei. Charged-current interactions of muonic neutrinos produce muons in the detector. The background of atmospheric muons is strongly suppressed by absorption in the sea, and completely eliminated in the case of upward-going muons. Contained vertically upward-going muons can be measured for energies from 5 to 60 GeV, corresponding to L/E_ν of about 1250 to 100 km/GeV, respectively, if the muon takes half of the neutrino energy. For the Super-Kamiokande oscillation parameters ($\Delta m^2 = .0035\ eV^2$, $\sin^2 2\theta = 1$) [4)], the first dip in the survival probability occurs at 350 km/GeV, at the maximum of the ANTARES sensitivity. The minimum value of L/E_ν can be reduced to about 10 km/GeV if partially-contained muons are analyzed over the full upward-going hemisphere.

2. Detector design

A schematic of the future ANTARES detector is shown in figure 1. Each string is composed of standard segments consisting of three optical modules, a local control module and an electro-mechanical cable. The photo-multiplier tubes in the optical modules are oriented down at 45°. Special containers house calibration equipment. A string control module at the bottom of the string receives and transmits slow-control commands and data. The string-control modules from different strings are linked to a common junction box by electrical cables. A standard deep-sea telecommunications cable links the junction box to a shore station where the data are filtered and recorded. The 0.1 km^2 detector will consist of four 'dense' strings with 41 segments spaced vertically 8 m apart, and nine 'sparse' strings with 21 segments spaced 16 m apart. The total height of the strings is 420 m. The strings are placed in a spiral, with

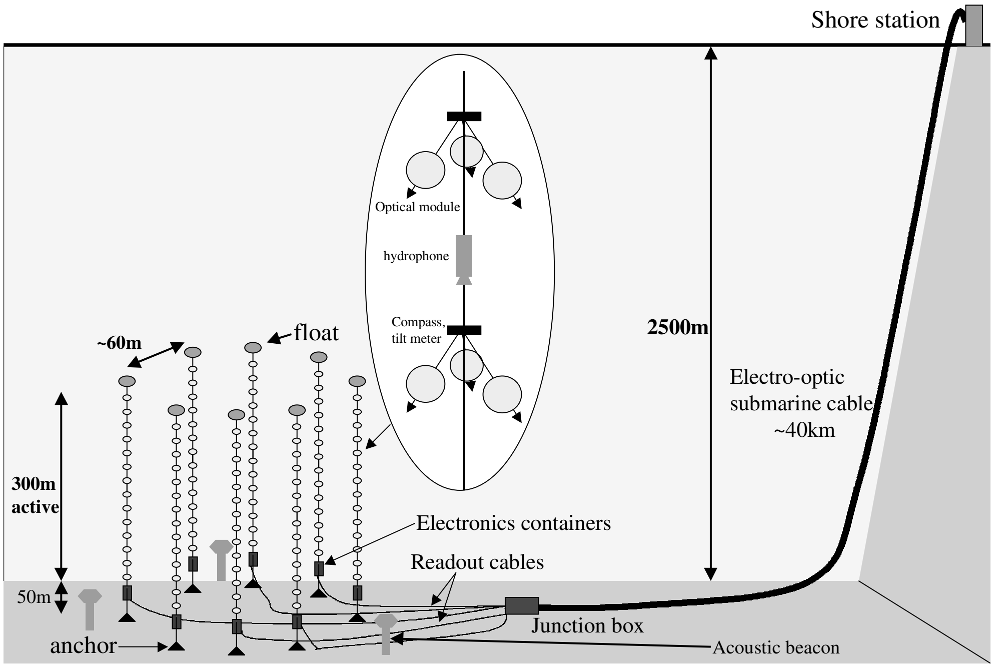

Fig. 1. Schematic diagram of the first phase of the ANTARES detector.

minimum horizontal spacing of 60 to 80 m.

The off-shore electronics is based on front-end digitization and digital data transmission. An ASIC called the Analogue Ring Sampler (ARS) is under development. For single-photo-electron pulses (99% of the photo-multiplier pulses), timing information will be stored in a pipeline memory until the second-level trigger arrives. For more complex signals, the chip samples the signal and holds an analog wave form on 128 switched capacitors. The 8-bit dynamic range can be increased to between 14 and 20 bits by reading out one or two of the dynode outputs in addition to the anode signal.

The off-shore trigger logic will be as simple and flexible as possible. The first-level trigger requires a coincidence of two of the three optical modules serviced by a single local control module. The second-level trigger is based on combinations of the first-level triggers. If a second-level trigger occurs, the full detector will be read out. The third-level trigger will be made in a farm of processors on shore. The first-level trigger rate will be about 150 kHz and the second-level rate a few kHz. The third level will select about 100 Hz of events to be recorded for off-line analysis.

3. Site characterization

A suitable site for a neutrino telescope requires deep, transparent water and proximity to shore facilities. A site 20 nautical miles off the French Mediterranean coast, near Toulon, at a depth of 2400 m has been explored. Optical background, biological fouling of optical surfaces, undersea currents, and meteorological conditions have been studied at this site, using special test strings. A low level background rate varying from 20 to 47 kHz was measured with an 8-inch Hamamatsu photo-multiplier tube housed in a 17-inch pressure-resistant Benthos glass sphere. Bursts of luminescence lasting about one second and giving peak counting rates up to several MHz were observed, correlated with the speed of the undersea currents [5)]. Fouling of the optical surfaces depended on the orientation, with lower rates for downward-looking surfaces. For vertical surfaces, the transmission loss after one year is about 1.5% [5)].

Different systems have been used to measure the water transparency. Initially, the light attenuation as a function of the distance from the source was measured using a 350 m long mooring string incorporating a 33 m long rigid structure holding an optical module at one end facing a motorized trolley carrying a light source along the structure. Continuous light sources (LEDs) emitting at different wavelengths were used. The attenuation length for blue light (466 nm wavelength) was measured to be $41 \pm 1 \pm 1$ m.

Light scattering was measured using a pulsed isotropic light source. The source consists of a set of six blue LEDs arranged along three perpendicular axes and placed at the centre of a Benthos sphere whose inner surface has been sanded. The deviation from isotropy was measured to be less than 20%. The intensity of the source

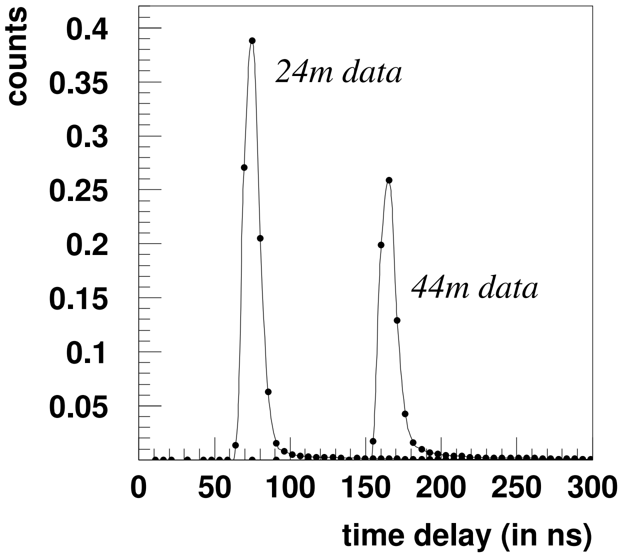

Fig. 2. Distribution of arrival times of photons for a distance between the detector and the source of 24 m (left) and 44 m (right). The 24 m distribution is normalized to 1, and the 44 m distribution is normalized relatively to the 24 m distribution.

was tuned so that only a few percent of the pulses would give rise to more than a single photoelectron at the detector. A TDC was started by the LED pulser and stopped by a photomultiplier tube signal. A special optical module using a 1-inch diameter photomultiplier tube was built in order to minimize accidental stops due to background light. Each run consisted of pulsing the light source at 10 kHz for 100 s and storing the distribution of times of arrival in a histogram.

The configuration of the setup consisted of two frames holding the light source and the optical module linked by three cables either 44 m or 24 m long.

Figure 2 shows the result of the measurement. The distribution corresponding to 24 m is normalized to 1 and the same normalization is applied to the distribution corresponding to 44 m. These data are presently being analysed in order to extract the scattering length and $< cos\theta >$ where θ is the scattering angle. From the raw data it can already be seen that at 24 m (44 m), the ratio of scattered to direct photons is less than 5% (10%). This result means that the scattering of light will not be a limiting factor for the angular resolution of the telescope.

4. Prototype tests

Complete prototype strings have also been immersed to test deployment techniques, instrumentation, and slow controls. Twenty different deployment/recovery cycles have been completed. Two deployment techniques have been used: horizontal deployment, in which the full detector is laid out on the surface of the sea before the release of the anchoring weight, and vertical deployment, in which the anchor is the first item immersed. The dynamic forces are reduced in the horizontal deployment, but the positioning accuracy of the vertical deployment is better. The recovery of the string is activated by an acoustical signal from the surface which disconnects the string from its anchoring weight. The undersea electrical connection of the string-control modules to the junction box has been tested successfully by the IFREMER crew of the "Nautile" submarine during one of these operations.

A prototype string planned for immersion in Spring 1999 ('Line 5') is shown in figure 3. The 350 m string will be anchored on the sea floor and maintained vertically by a large buoy at the top of the string. It is composed of two cables supporting 16 optical module frames placed every 15 m starting from 95 m above the sea floor. Each of the 16 frames holds two 17-inch glass spheres with center-to-center separation of 1.6 m. Eight of the spheres will contain photo-multiplier tubes, oriented horizontally so that downward-going muons can be detected.

Line 5 will be equipped with a positioning system to allow the reconstruction of the position of each optical module on the string with a precision of about 10 cm. Tilt-meters and compasses will measure local tilt angles and orientations. They will be installed in titanium spheres on 12 of the optical module frames and in 6 of the un-equipped glass spheres. The string will also hold four range-finders communicating with four external transponders at fixed positions 200 m away on the sea floor to allow a precise 3D localisation of a few points on the string by acoustical triangulation. The string will be connected to a shore station 40 km away by means of an electro-optical cable. Slow control communications as well as experimental data will be sent over the four optical fibers in this cable. The slow-control network, based on an industrial field-bus technology (WorldFip), will control the power distribution, the readout electronics, the acoustic system, and the readout of sensor data.

5. Detector performances

A software package has been developed to simulate neutrino interactions in the medium surrounding the detector, particle tracking and Cherenkov light emission. The response of the detector to the various types of physics events has been studied mainly using a version of the DADA program [6] which originated in the Baïkal col-

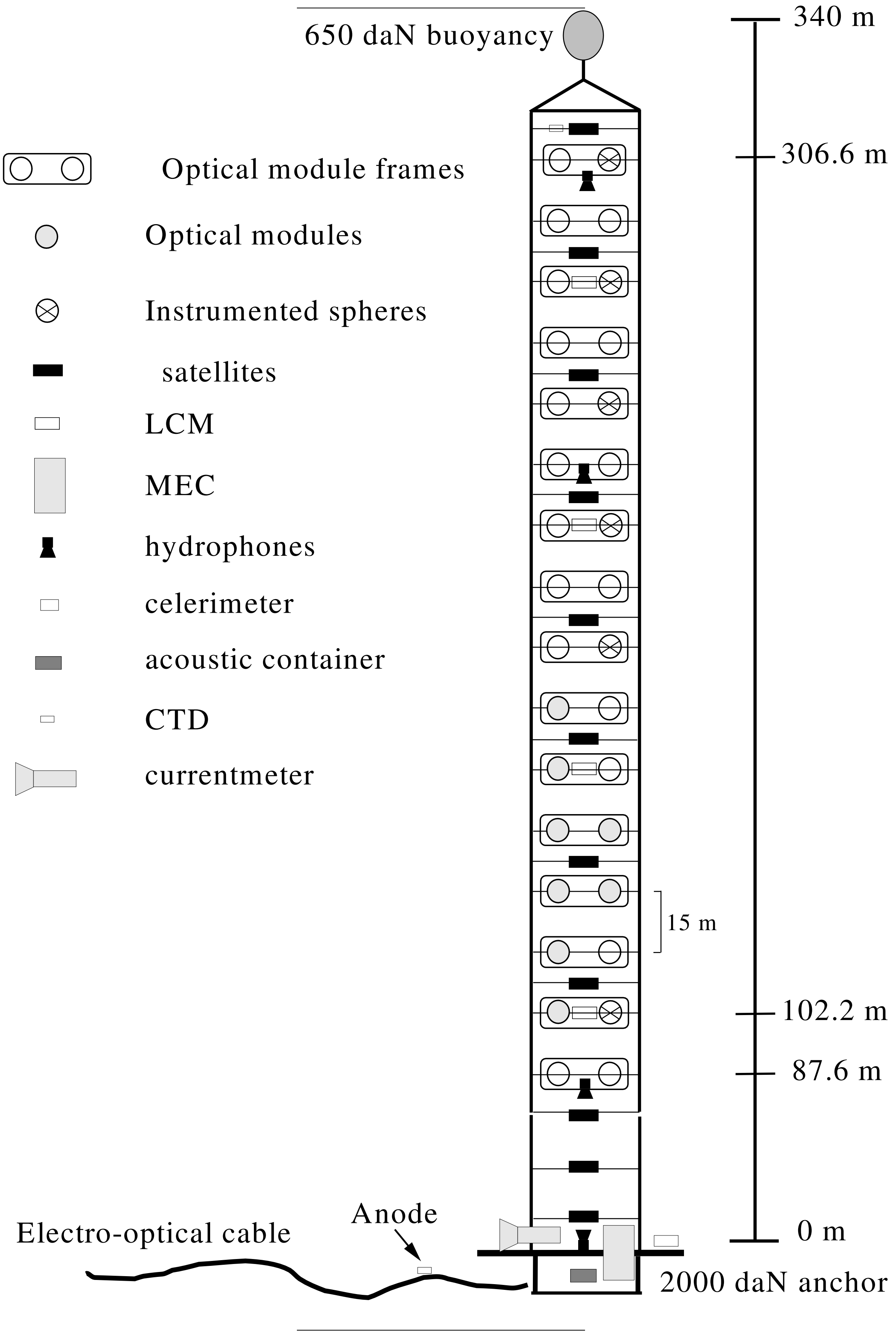

Fig. 3. Schematic view of the line 5 prototype.

laboration. We have modified this programme for the ANTARES detector and have also made modifications to improve the performance at high energies.

All simulated events include random hits from ^{40}K in the sea water. The string deformation due to the currents has also been simulated. The event reconstruction is made by using the position and the recorded time for each hit OM. A filter has been developed to remove parasitical hits due to ^{40}K. The angular resolution depends on the timing accuracy. The overall timing accuracy is a quadratic sum of the PMT timing error, the error of the OM position (typically 10 cm) and the error of clock synchronisation (expected to be better than 1 ns). The angular resolution for neutrinos with a $1/E_\nu^2$ spectrum is estimated to be 0.2 degrees.

Above 1 TeV the muon energy can be estimated by an algorithm which combines the reconstructed trajectory and the sum of the recorded pulse heights. The error on the energy is a factor of 3 for energies below 10 TeV and a factor of 2 for energies above 10 TeV. Below 100 GeV the muon energy is estimated by measuring its range.

5.1. Astrophysics

Figure 4 shows the effective detector area as a function of the true energy for muons induced by high energy neutrinos which trigger the detector, for those which are reconstructed and for those which satisfy our selection criteria. Different models predict diffuse neutrino fluxes from active galactic nuclei (AGN) which could dominate the atmospheric neutrino flux at energies above 10-100 TeV. The event rates expected for these neutrino fluxes and for atmospheric neutrinos have been estimated for events which satisfy our selection criteria and are given in table 1 for 10 TeV and 100 TeV thresholds on the reconstructed energy.

Moreover, due to the extremely low angle between the muon and the parent neutrino and to the good quality of the muon direction measurement, the atmospheric neutrino background contaminating each source can be reduced to a very low level by selecting very small angular regions of the sky. In that way, a signal of only a few events could be significant. The sensitivity of the detector to muon neutrinos can be estimated from measured low-energy gamma-ray fluxes by assuming that *i)* the low energy gamma-rays are of hadronic origin and *ii)* the emitted gamma-rays have a differential energy spectrum E^{-2}.

Using the 2nd EGRET catalog for sources measured during the P12 period, the derived neutrino flux has been extrapolated to the energies where the ANTARES neutrino detector is sensitive.

The detection of the most luminous individual sources could require more than one year of data acquisition. Nevertheless, a statistically significant effect could be detected in one year by adding the contributions of all the extra-galactic sources. The expected number of events is between ten and about one hundred (depending on the value of the differential spectral index used: 2 or 2.2) to be compared to a total

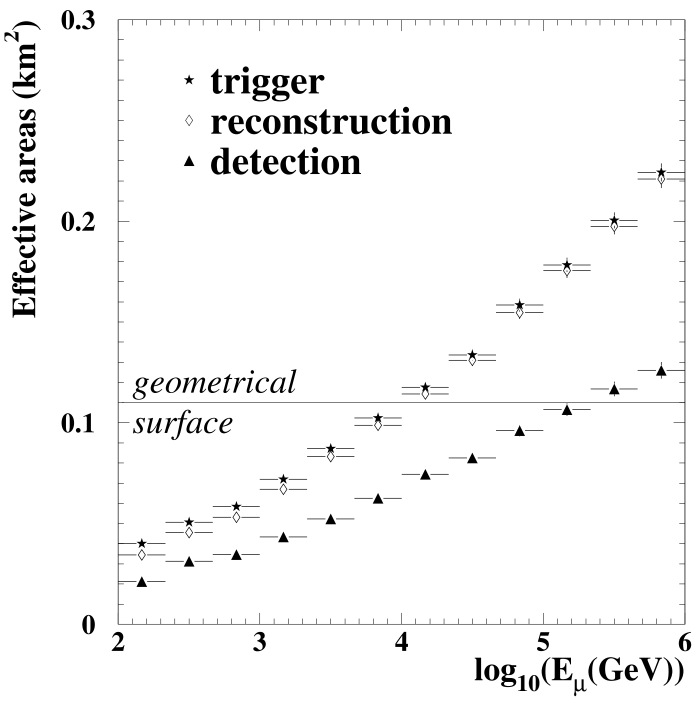

Fig. 4. Effective area for triggering, reconstructed and selected events. The areas are averaged for muons coming from the lower hemisphere.

Table 1. Number of accepted muons reconstructed as upward-going above the estimated energy E_μ^{rec} per year. The errors are statistical.

Model	$\mathbf{E}_\mu^{\mathrm{rec}} \geq$ 10 TeV	$\mathbf{E}_\mu^{\mathrm{rec}} \geq$ 100 TeV
Atmospheric		
ATM [7]	68±13	0.8±0.1
Generic AGN models		
SDSS [1]	251±12	134±10
NMB [8]	217±9	64±4
Blazars		
PRO [9]	34±2	21±2
MRLB [10]	7.8±0.4	2.6±0.3

background of about 3 events.

The search for neutrinos from sources of gamma ray bursts uses the narrow space and time window from the gamma ray information. Here, there is negligible background. With the flux given by Waxman and Bahcall [11] and the effective detector area shown in figure 4, the rate expected is $\simeq 10$ signal events per year with a background rate of less than 0.001 event per year.

5.2. Neutrino oscillations

The measurement of the atmospheric neutrino flux for energies below 100 GeV will allow us to study neutrino oscillations for values of neutrino mass difference Δm^2 between 10^{-3} and 10^{-2} eV^2. An analysis has been carried out using simulated interactions to explore the sensitivity of the proposed experiment to the neutrino oscillation parameters Δm^2 and $\sin^2 2\theta$. The simulation used the expected experimental acceptance and the known flux of atmospheric neutrinos. The analysis is based on semicontained events, using the energy visible in the detector for the muon energy. The neutrino flight distance L is related to the zenith angle of the track, θ_z, by $L \sim L_0 \cos\theta_z$, where L_0 is the diameter of the earth, 12740 km.

The histogram in figure 5 shows the distribution of accepted events as a function of $E_\mu/(L_\mu/L_0)$, where E_μ is the energy and L_μ the oscillation length corresponding to the reconstructed muon tracks. This histogram represents a simulation of three years of operation, without neutrino oscillations. The "data" points in figure 5 represent the same simulated events, but with each event weighted with the probability $P = 1 - \sin^2 2\theta \sin^2 (1.27\Delta \mathrm{m}^2 \mathrm{L}_\nu/\mathrm{E}_\nu)$, using the true neutrino values of E_ν and L_ν.

To explore the Δm^2 and $\sin^2 2\theta$ parameter space, a series of three-year simulations was carried out as just described, each one producing a distribution like the one shown by the crosses in figure 5. Each of these distributions was compared with a high-statistics simulation without oscillations. To remove the effect of absolute normalization, the no-oscillations distribution was multiplied by a factor which was varied as a free parameter. For each point in parameter space a large number of such simulations was carried out. Figure 6 shows the region of parameters where neutrino oscillations could be excluded at 90% of confidence level (CL) in 80% of simulated experiments.

It is important to note that the present analysis is exploratory and can be refined in many ways. The ν_μ quasi-elastic events (estimated to about 15% of the charged current ν_μ events) were not included in these simulations. These low energy events have a better correlation between the produced muon and the parent neutrino energy than the deep-inelastic events used here. Inclusion of these events will improve the experimental sensitivity to low Δm^2. On the other hand, the sensitivity will suffer in the real experiment due to systematics resulting from variations in the detector

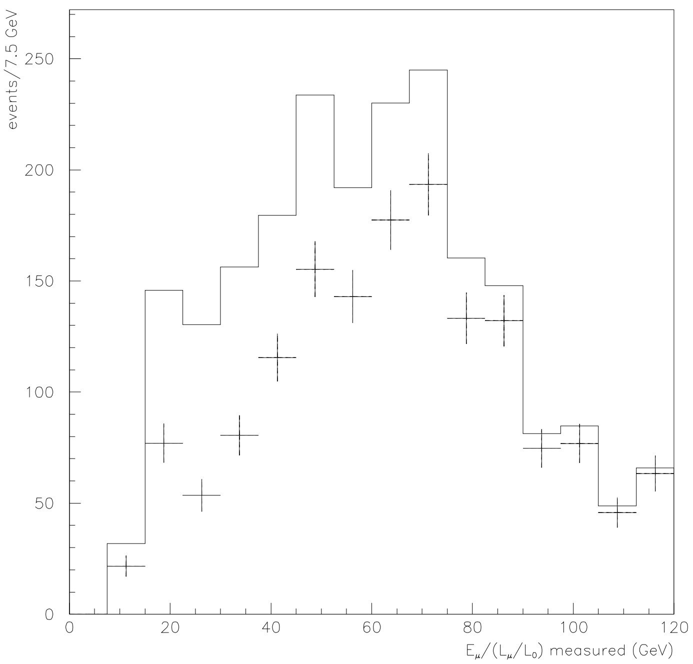

Fig. 5. Simulated number of events in 3 years with no oscillations (histogram) and with oscillations for $\sin^2 2\theta = 1.0$ and $\Delta m^2 = 0.0035$ eV^2 (points).

acceptance and assumptions about the neutrino flux and its energy and angular dependence and about backgrounds.

The backgrounds have so far not been taken into account in the analysis. However, making a known background subtraction with the magnitude of backgrounds presently estimated would have little impact on the results. The backgrounds from ν_e and from non-contained ν_μ are related to the atmospheric flux and are well simulated, so a background subtraction can be made. The present simulations indicate the backgrounds from muons originating in the atmosphere are small. These simulations must be refined by including light diffusion in the water, and extended to higher statistics. The detector will have a significant acceptance for events above the horizontal, and these events can be used to control the muon background simulations for events below the horizontal.

6. Conclusions

Most of the technical aspects relating to the construction and operation of an underwater neutrino telescope have been addressed within the ANTARES project.

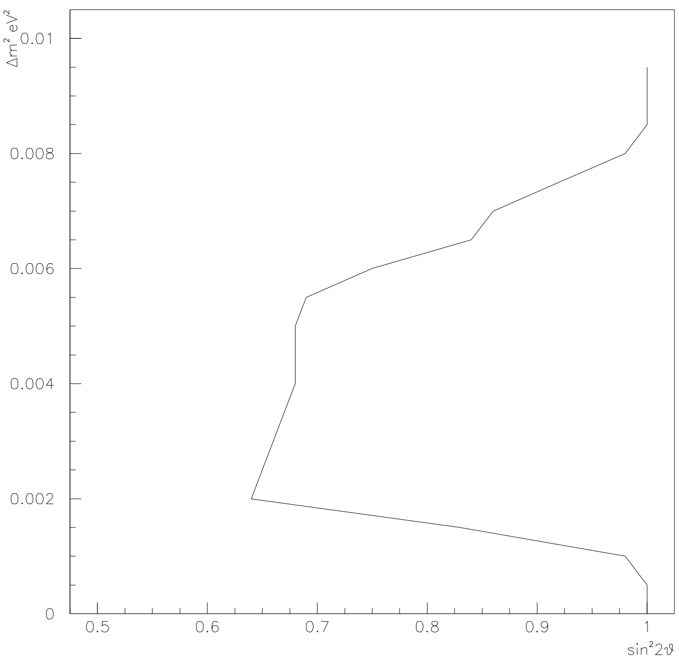

Fig. 6. For three years of data taking, the region where neutrino oscillations could be excluded at 90% of CL in 80% of simulated experiments..

The program of the site evaluation has shown that the quality of the environmental parameters is quite satisfactory to consider the construction of the next stage detector consisting of $\simeq$1000 optical modules covering a detector area of $\simeq 0.1\,\mathrm{km}^2$.

The scientific programme includes neutrino astronomy, indirect detection of non-baryonic dark matter and the search for neutrino oscillations. Due to the very good angular resolution, the atmospheric neutrino background can be reduced to very low values allowing the detection of signals from AGNs and from sources of gamma ray bursts.

The analysis of low energy ($< 50\,\mathrm{GeV}$) events will allow the study of the neutrino oscillations in a region of Δm^2, $\sin^2 2\vartheta$ which fits with the recent values reported by the Super-Kamiokande experiment.

7. References

1) F. W. Stecker et al., *Phys. Rev. Lett.* **66** (1991) 2697;
(Errata, *Phys. Rev. Lett.* **69** (1992) 2738).

2) G. Jungman, M. Kamionkowski and K. Griest, *Phys. Rep.* **267** (1996) 195.
3) J. Edsjö, in *Aspects of neutrino detection of neutralino dark matter*, Ph.D. thesis, University of Uppsala, 1997.
4) Y. Fukuda, *Phys. Rev. Lett.* **81** (1998) 1562.
5) L. Moscoso, in *Neutrino telescopes under the ocean: The case for ANTARES* Talk given at the Neutrino98 Conference, Takayama, Japan, July 4-9, 1998.
6) C. Wiebusch, in *The Detection of Faint Light in Deep Underwater Neutrino Telescopes*, Ph. D. Thesis, PITHA 95/37, RWTH-Aachen (1995).
7) L. V. Volkova, *Sov. J. Nucl. Phys.* **31** (1980) 1510.
8) L. Nellen, K. Mannheim and P. L. Biermann, *Phys. Rev.* **D47** (1993) 5270.
9) R. J. Protheroe1996, in *High Energy Neutrinos from Blazars*, ADP-AT-96-7 and astro-ph/9607165, 1996.
10) K. Mannheim, *Astrop. Phys.* **3** (1995) 295.
11) E. Waxman and J. Bahcall, *Phys. Rev.* **D59** (1999) 023002.